THE JOURNAL OF BIOLOGICAL CHEMISTRY VOL. 286, NO. 9, pp. 7202–7213, March 4, 2011

Expression and Function of Human MRP1 (ABCC1) Is Dependent on Amino Acids in Cytoplasmic Loop 5 and Its Interface with Nucleotide Binding Domain 2*

Received for publication, July 22, 2010, and in revised form, November 22, 2010 Published, JBC Papers in Press, December 20, 2010, DOI 10.1074/jbc.M110.166959

Surtaj H. Iram and Susan P. C. Cole[1]

From the Division of Cancer Biology and Genetics, Queen's University Cancer Research Institute, Kingston, Ontario K7L 3N6, Canada

Multidrug resistance protein 1 (MRP1) is an ATP-binding cassette transporter that effluxes drugs and organic anions across the plasma membrane. The 17 transmembrane helices of MRP1 are linked by extracellular and cytoplasmic loops (CLs), but their role in coupling the ATPase activity of MRP1 to the translocation of its substrates is poorly understood. Here we have examined the importance of CL5 by mutating eight conserved charged residues and the helix-disrupting Gly^{511} in this region. Ala substitution of Lys^{513}, Lys^{516}, Glu^{521}, and Glu^{535} markedly reduced MRP1 levels. Because three of these residues are predicted to lie at the interface of CL5 and the second nucleotide binding domain (NBD2), a critical role is indicated for this region in the plasma membrane expression of MRP1. Further support for this idea was obtained by mutating NBD2 amino acids His^{1364} and Arg^{1367} at the CL5 interface, which also resulted in reduced MRP1 levels. In contrast, mutation of Arg^{501}, Lys^{503}, Glu^{507}, Arg^{532}, and Gly^{511} had no effect on MRP1 levels. Except for K503A, however, transport by these mutants was reduced by 50 to 75%, an effect largely attributable to reduced substrate binding and affinity. Studies with ^{32}P-labeled azido-ATP also indicated that whereas ATP binding by the G511I mutant was unchanged, vanadate-induced trapping of azido-ADP was reduced, indicating changes in the catalytic activity of MRP1. Together, these data demonstrate the multiple roles for CL5 in the membrane expression and function of MRP1.

Multidrug resistance protein 1 (MRP1/ABCC1) is an integral membrane protein belonging to the ATP-binding cassette (ABC)[2] superfamily of transport proteins (1, 2). When overexpressed in tumor cells, MRP1 confers resistance to anticancer drugs and other xenobiotics of remarkable structural diversity, including oxyanions containing arsenic and antimony (3–5). In addition to cytotoxic agents, MRP1 mediates the ATP-dependent efflux of a variety of organic anions derived from both endogenous metabolites and exogenous xenobiotics, many of which are conjugated to glutathione (*e.g.* the cysteinyl leukotriene (LTC_4)) or glucuronide (*e.g.* estradiol glucuronide ($E_2 17\beta G$)) (4–6). In some instances, a role has been established for MRP1 in influencing the *in vivo* disposition of these compounds (4, 7, 8).

Eukaryotic ABC proteins typically have a four-domain core structure, composed of two hydrophobic membrane-spanning domains (MSDs), each with six transmembrane (TM) α-helices, and two cytoplasmic nucleotide binding domains (NBDs). Several ABCC subfamily members, including MRP1, have an additional, third MSD (MSD0) that precedes the four-domain core structure (Fig. 1*A*) (1, 8, 9). The two NBDs of ABC proteins coordinate in a head-to-tail orientation to form a "sandwich" dimer that comprises two composite nucleotide binding sites, which bind and hydrolyze ATP to provide the energy necessary for the transport process (10). On the other hand, the 12 intertwined TM α-helices of the core MSD1 and MSD2 form the substrate translocation pathway and are brought into close proximity to the NBDs through the cytoplasmic loops (CLs) that connect the TMs (Fig. 1*B*) (10, 11). It is now widely accepted that the CLs mediate the coupling of the ATPase (catalytic) activity at the nucleotide binding sites to substrate translocation through the MSDs (10, 12).

Although a number of amino acids in or proximal to the TMs have been characterized as critical for the activity and/or substrate specificity of MRP1 (6, 13–15), there are few comparable analyses of the CLs of this transporter. Studies of the CLs of several other mammalian ABC proteins, however, have identified a number of functionally important amino acids. For example, Kwan and Gros (16) identified several CL1 mutants of murine P-glycoprotein (Abcb1a) that exhibit a partial or complete loss of drug transport activity. In addition, a recent study on the transporter associated with antigen processing (TAP; ABCB2/3) demonstrated that specific residues in CL1 and CL2 of TAP1 were important for both peptide binding and translocation (17). Furthermore, many disease-associated mutations are located in the CLs of the cystic fibrosis transmembrane conductance regulator (CFTR) (*ABCC7*), which cause it to be retained in the endoplasmic reticulum (18, 19). Finally, a naturally occurring mutant of CFTR in which 19 amino acids are absent from the CL linking TM4 to TM5 is very poorly expressed, suggesting a role for this region in the proper folding and/or membrane trafficking of this chloride channel (20).

* This work was supported by Grant MOP-10519 from the Canadian Institutes of Health Research.

[1] Holds the Canada Research Chair in Cancer Biology and the Bracken Chair in Genetics and Molecular Medicine. To whom correspondence should be addressed. Fax: 613-533-6830; E-mail: spc.cole@queensu.ca.

[2] The abbreviations used are: ABC, ATP-binding cassette; MRP, multidrug resistance protein; MSD, membrane-spanning domain; TM, transmembrane helix; CL, cytoplasmic loop; NBD, nucleotide binding domain; LTC_4, leukotriene C_4; $E_2 17\beta G$, 17β-estradiol-17-β-(D-glucuronide); CFTR, cystic fibrosis transmembrane conductance regulator; ERAD, endoplasmic reticulum-associated degradation.

With respect to MRP1, we demonstrated previously the functional importance of several amino acids in CL7, which connects TM15 to TM16 in MSD2 (Fig. 1*A*). Thus, mutation of the adjacent Tyr residues at positions 1189 and 1190 decreases MRP1 transport activity, especially with respect to the transport of the tripeptide antioxidant glutathione (21). Furthermore, substitutions of several charged amino acids in CL7 substantially reduce the plasma membrane expression of MRP1 (*i.e.* Arg^{1166} and Asp^{1183}), cause substrate-selective changes in its transport activity (*i.e.* Asp^{1179} and Glu^{1144}), or do both (*i.e.* Lys^{1141}) (22, 23).

Homology models of the nucleotide-bound core structure of human MRP1 predict that a stretch of amino acids parallel to the membrane at the bottom of CL7 of MSD2 is in close proximity to the first NBD (NBD1), whereas the analogous region in CL5 of MSD1 is in contact with the second NBD (NBD2) (Fig. 1*B*) (11). Based on the apparent 2-fold symmetry of the MRP1 core structure, it might reasonably be assumed that CL5 and CL7 would serve similar coupling functions in this and possibly related ABCC transporters. However, this assumption may not be correct, as it is now well established that the NBDs of MRP1 are functionally asymmetric, with most of the catalytic (ATP-hydrolyzing) activity residing in NBD2 (24, 25). The CLs of MSD2 also contain several conserved Pro residues that are not present in the CLs of MSD1 (26). Because of the α-helical disrupting properties of Pro, this difference may result in differences in the geometry and/or mobility of CL4 and CL5 in MSD1 *versus* CL6 and CL7 in MSD2. Finally, although both CL5 and CL7 contain a high proportion of charged amino acids, these are more frequently conserved in CL5 than in CL7.

The apparent asymmetries in the sequence and function of the two halves of MRP1 have prompted us to extend our analyses of the CLs of MRP1 by investigating the functional importance of the eight most conserved charged amino acids in CL5. We also investigated Gly^{511} because of its possible role in influencing the geometry and/or mobility of CL5, and thus its potential to affect the coupling interactions of this region with NBD2.

EXPERIMENTAL PROCEDURES

Materials—[14,15,19,20-^{3}H]LTC_4 (158 Ci mmol^{-1}) and [6,7-^{3}H]$E_2$17βG (45 Ci mmol^{-1}) were purchased from PerkinElmer Life Sciences, and 8-azido-[α-^{32}P]ATP (12.6 Ci mmol^{-1}) was from Affinity Photoprobes (Lexington, KY). LTC_4 was purchased from Calbiochem, and $E_2$17βG, nucleotides, phenylmethylsulfonyl fluoride, phosphate-buffered saline, sodium orthovanadate, NaF, $BeSO_4$, DAPI, dithiothreitol, and 2-mercaptoethanol were from Sigma.

Site-directed Mutagenesis—Site-directed mutagenesis was performed using *Pfu* Turbo DNA polymerase (Stratagene) according to the manufacturer's instructions with mutagenic primers (Integrated DNA Technologies, Inc., Coralville, IA). The MRP1 expression vector pcDNA3.1(−)-$MRP1_k$ has been described previously (27). To generate point mutations in CL5, plasmid pBluescriptSK(+)BamHI/SpHI-MRP1 containing a 1.9-kb fragment from pcDNA3.1(−)-$MRP1_k$ was used as the template with the following mutagenic primers (substituted nucleotides are underlined): R501A, 5′-GAG CAA AGA CAA TGC GAT CAA GCT GAT G-3′; K503A, 5′-GAC AAT CGG ATC GCG CTG ATG AAC G-3′; E507A, 5′-GCT GAT GAA CGC AAT TCT CAA TGG G-3′; G511I, 5′-CTC AAT ATT ATC AAA GTG CTA AAG CTT TAT GCC TGG GAG CTG GC-3′; K513A, 5′-CTC AAT GGG ATC GCA GTG CTA AAG C-3′; K513R, 5′-CTC AAT GGG ATC AGA GTG CTA AAG C-3′; K516A, 5′-GAT CAA AGT GCT AGC GCT TTA TGC CTG-3′; K516R, 5′-GAT CAA AGT GCT AAG ACT TTA TGC CTG-3′; E521A, 5′-CTT TAT GCC TGG GCG CTG GCA TTC-3′; E521D, 5′-CTT TAT GCC TGG GAC CTG GCA TTC-3′; R532A, 5′-GTG CTG GCC ATT GCG CAG GAG GAG CT-3′; E535A, 5′-CAT CAG GCA GGA GGC CTT GAA GGT GCT GAA G-3′; and E535D, 5′-CAG GCA GGA GGA TCT GAA GGT GCT GAA G-3′. After confirmation of mutation by sequencing, a 657-bp PshAI/Bsu36I fragment containing the desired mutation was subcloned back into pcDNA3.1(−)-$MRP1_k$, and the integrity of the sequence was confirmed by sequencing.

To create the CL6 mutation H1049A, a 2-kb XmaI fragment (containing nucleotides 2337–4322) in pGEM-3Z (Promega, Madison, WI) was used as the template with the mutagenic primer 5′-CCG CTG TCT GGC CGT GGA CCT GC-3′. After confirming the mutation by sequencing, a 0.4-kb Eco47III/NcoI fragment containing the desired mutation was subcloned into pGEM-3Z-XmaI/MRP1, and then a 1.5-kb BsmBI/ClaI fragment containing the desired mutation was subcloned back into pcDNA3.1(−)-$MRP1_k$.

To engineer mutations of His^{1364} and Arg^{1367} in NBD2, a 0.8-kb EcoRI/KpnI fragment of MRP1 in pBluescriptSK(+) was used as the template with the following mutagenic primers (substituted nucleotides are underlined): H1364A, 5′-GAT CGG CCT GGC CGA CCT CCG C-3′; and R1367A, 5′-CTG CAC GAC CTC GCC TTC AAG ATC AC-3′. After sequence confirmation, the 0.8-kb EcoRI/KpnI fragment was moved back into pcDNA3.1(−)-$MRP1_k$ and sequenced again to confirm the integrity of the sequence and the presence of the mutations.

Transfection of MRP1 Expression Vectors and Preparation of Membrane Vesicles—Wild-type and mutant pcDNA3.1(−)-MRP1 expression vectors were transfected into SV40-transformed human embryonic kidney cells (HEK293T) (27). Cells (18×10^6) were seeded in 150-mm plates and transfected 24 h later (at 90–95% confluency) with 20 μg of plasmid DNA using Lipofectamine 2000 (Invitrogen) according to the manufacturer's instructions. After 48 h, the HEK293T cells were harvested, and membrane vesicles were prepared as described previously (27). The total protein content of the vesicles was quantified using a Bio-Rad Bradford assay with bovine serum albumin as a standard. Untransfected cells and cells transfected with a wild-type MRP1 cDNA expression vector were included as controls in all experiments.

Measurements of MRP1 Protein Levels in Transfected Cells—The levels of wild-type and mutant MRP1 proteins were determined by immunoblot analysis using the human MRP1-specific murine mAb QCRL-1 (diluted 1:5,000–1:10,000), which detects an epitope defined by amino acids 918–924 essentially as described (28). To confirm equal load-

ing of protein in some experiments, blots were probed with a murine mAb against α-tubulin (2 mg ml^{-1}) (Sigma-Aldrich). Densitometry of immunoblots was performed using ImageJ software.

Confocal Microscopy—HEK293T cells were seeded at 5×10^5 cells/well in a 6-well plate on coverslips coated with 0.1% gelatin in Dulbecco's modified Eagle's medium containing 7.5% fetal bovine serum. Twenty-four h later, cells were transfected with the MRP1 constructs as before; and 48 h later, the coverslips were washed with PBS, and cells were fixed with 95% ethanol, washed in PBS, and permeabilized by adding 0.2% Triton X-100 in PBS. Cells were blocked with three changes over 45 min of blocking solution (0.1% Triton X-100 and 2% bovine serum albumin in PBS) and then incubated with the human MRP1-specific rat mAb, MRPr1 (defined by amino acids 238–247; diluted 1:1500), and a mouse mAb against calnexin (diluted 1:75) in blocking solution for 60 min at 37 °C (28, 29). The coverslips were washed in PBS and incubated for 60 min at 37 °C with Alexa Fluor 546 goat anti-rat IgG (H+L) $(Fab')_2$ fragment (diluted 1: 500) and Alexa Fluor 488 goat anti-mouse IgG (H+L) $(Fab')_2$ fragment (diluted 1: 500) in blocking solution, washed again, and then placed on slides containing SlowFade® antifade solution (Molecular Probes, Inc., Eugene, OR) and DAPI (2.5 mg ml^{-1}, diluted 1:100 in antifade solution). Cells were examined using a Leica TCS SP2 MS multiphoton system confocal microscope (Leica Microsystems, Heidelberg, Germany).

MRP1-mediated Transport of ^{3}H-Labeled Substrates by Membrane Vesicles—ATP-dependent uptake of ^{3}H-labeled substrates by the membrane vesicles was measured using a rapid filtration method (30) adapted to a 96-well microtiter plate format (31). In brief, 2 μg of membrane vesicle protein was incubated with 50 nM/10 nCi [^{3}H]LTC_4 for 1 min at 23 °C or 400 nM/20 nCi [^{3}H]$E_2$17βG for 1 min at 37 °C in a 30-μl reaction mixture containing 10 mM $MgCl_2$ and 2 mM AMP or 2 mM ATP in transport buffer (250 mM sucrose and 50 mM Tris-HCl, pH 7.4) with an ATP-regenerating system consisting of 100 μg ml^{-1} creatine kinase and 10 mM creatine phosphate. MRP1-mediated uptake was stopped after 1 min by rapid dilution in ice-cold transport buffer, and reactions were filtered through a Unifilter-96 GF/B plate (PerkinElmer Life Sciences) using a Packard Filtermate Harvester. Tritium associated with the vesicles was counted, and ATP-dependent uptake was calculated by subtracting the uptake in the presence of AMP from the uptake measured in the presence of ATP. Unless specified otherwise, all transport assays were carried out in triplicate, and results were expressed as means ± S.D. and corrected for any differences in expression of the mutant MRP1 proteins relative to wild-type MRP1.

In competition transport experiments, the same conditions were used as described above, except that membrane vesicles were preincubated for 15 min on ice with different concentrations of unlabeled $E_2$17βG (0, 12.5, 25, and 50 μM) or LTC_4 (0, 300, 600, and 900 nM) before proceeding with the transport assays.

*Kinetic Analysis of [^{3}H]$E_2$17βG Transport*—K_m and V_{max} values for $E_2$17βG uptake by membrane vesicles (4 μg) were determined by measuring ATP-dependent uptake at eight different $E_2$17βG concentrations (0.25–25 μM) for 1 min at 37 °C in 50 μl of transport buffer containing components as described above. Data were analyzed using GraphPad Prism™ software, and kinetic parameters were calculated by nonlinear regression and Michaelis-Menten analyses.

Photolabeling of MRP1 by [^{3}H]LTC_4—Wild-type and mutant MRP1 membrane proteins were photolabeled with [^{3}H]LTC_4 essentially as described (22). Briefly, membrane vesicles prepared from HEK293T cells transfected with wild-type and mutant MRP1 cDNAs (50 μg of protein in 50 μl transport buffer) were incubated with [^{3}H]LTC_4 (120 nCi, 200 nM) and 10 mM $MgCl_2$ at room temperature for 30 min and then frozen in liquid nitrogen. Samples were then alternately irradiated at 302 nm for 1 min and snap-frozen 10 times in liquid N_2. Radiolabeled proteins (50 μg) were resolved by SDS-PAGE, and the gel was processed for fluorography. The gel was exposed to Bioflex® MSI film (InterScience, Troy, NY) for 3 days at −70 °C. Relative levels of photolabeling were estimated by densitometric analysis as described previously.

Photolabeling of MRP1 with 8-Azido-[α-^{32}P]ATP—Wild-type and mutant MRP1 proteins from transfected cells were photolabeled with 8-azido-[α-^{32}P]ATP essentially as described previously (26). Membrane vesicles (20 μg of protein) were dispersed in 20 μl of transport buffer containing 5 mM $MgCl_2$ and 5 μM 8-azido-[α-^{32}P]ATP. After 5 min incubation on ice, the samples were cross-linked at 302 nm for 8 min, washed, and then solubilized in Laemmli buffer and subjected to SDS-PAGE. After drying, the gel was exposed to film for 2–4 h.

Orthovanadate- and Beryllium Fluoride-induced Trapping of 8-Azido-[α-^{32}P]ADP—To measure orthovanadate-induced trapping of 8-azido-[α-^{32}P]ADP by MRP1, membrane proteins (20 μg) were incubated in transport buffer (20 μl) containing 5 mM $MgCl_2$, 1 mM freshly prepared sodium orthovanadate, and 5 μM 8-azido-[α-^{32}P]ATP at 37 °C for 15 min (26). To measure trapping induced by beryllium fluoride, a mixture of 1 mM NaF and 200 μM $BeSO_4$ in transport buffer was added instead of sodium orthovanadate (32). The reactions were stopped by the addition of ice-cold Tris-EGTA buffer, and membrane proteins were washed and resuspended before cross-linking at 302 nm as described previously (26). Membrane vesicles were then solubilized in Laemmli buffer and subjected to SDS-PAGE, and after drying, gels were exposed to film for 12–24 h.

RESULTS

Sequence Alignment and Location of CL5 Residues Targeted for Mutagenesis—Our recent homology models of the core structure of MRP1 developed based on the crystal structure of nucleotide-bound Sav1866 from *Staphylococcus aureus* indicate that the α-helices containing TM9 and TM10 extend into the cytoplasm to become what we have designated as CL5 (Fig. 1, *A* and *B*) (11). The model also indicates that CL5 in MSD1 and CL6 in MSD2 come close together and form an interface with NBD2. This configuration is conserved in the recently reported crystal structure of nucleotide-free murine P-glycoprotein (Abcb1) (33) and other Sav1866-based homol-

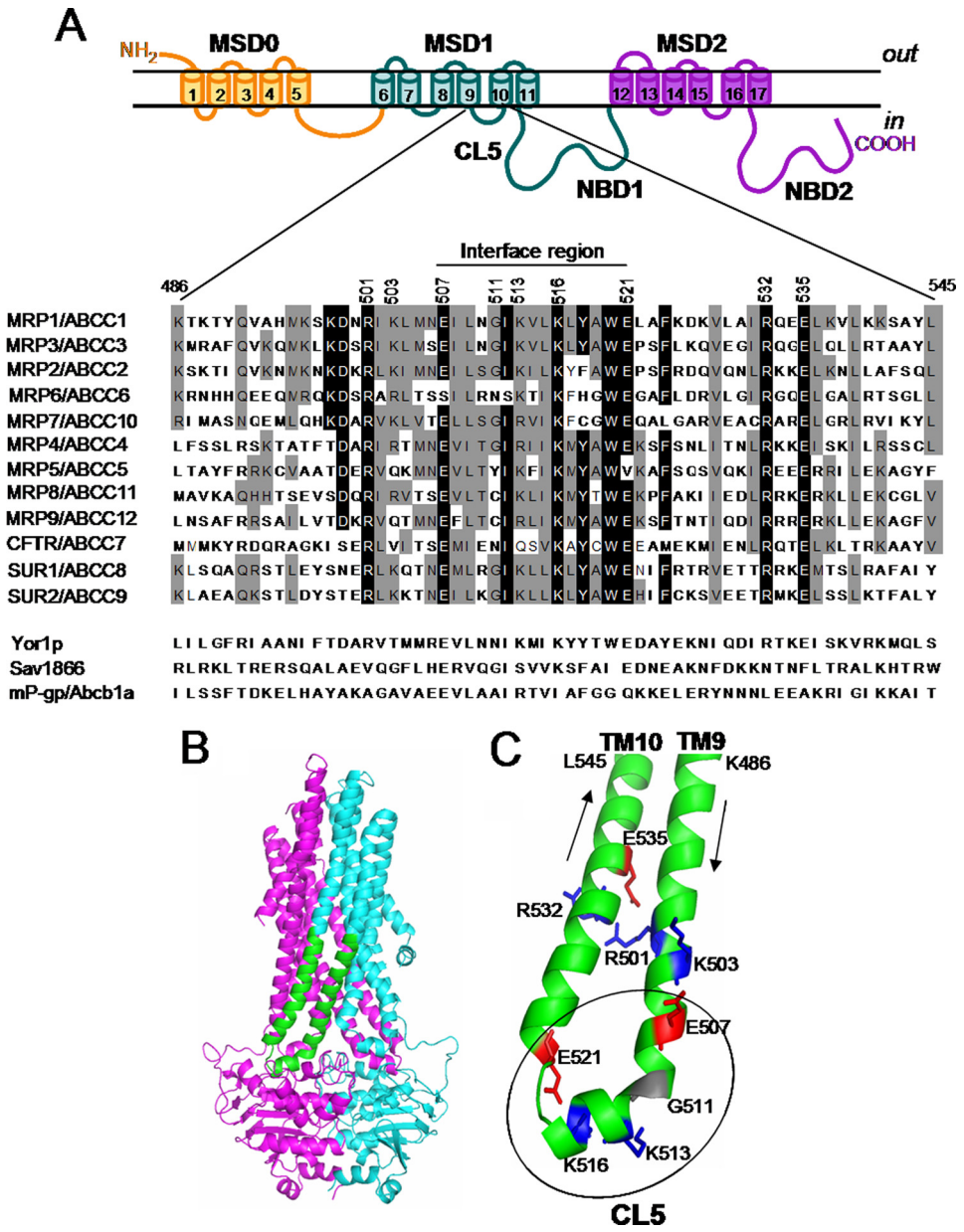

FIGURE 1. **MRP1 secondary structure, homology models and CL5 sequence alignments.** *A*, *top*, a predicted secondary structure of MRP1 showing the location of the CL5 (amino acids 486–545). *Bottom*, sequence alignments of MRP1 CL5 and analogous regions in human ABCC homologs, bacterial Sav1866, yeast Yor1p, and mouse P-glycoprotein generated using ClustalW. Amino acids that are identical in all human ABCC proteins are shown on a *black background*, whereas residues that are partially conserved are on a *gray background*. CL5 amino acids 507–521 predicted to form an interface with NBD2 in MRP1 are indicated with a *solid line* above the alignment. *SUR*, sulfonylurea receptor. *B*, location of CL5 (*green*) in a three-dimensional homology model of MRP1 (lacking MSD0) generated using the crystal structure of nucleotide-bound Sav1866 from *S. aureus* as template (11); MSD1 and NBD1 (*cyan*); and MSD2 and NBD2 (*magenta*). *C*, expanded CL5 region from the homology model showing the amino acids mutated in this study. The region of CL5 at the interface with NBD2 is *encircled*. *B* and *C* were created using PyMOL.

ogy models of mammalian ABC proteins proposed to date (10, 34–36).

The boundaries of CL5 vary to some degree depending on the algorithm used to predict the secondary structure of MRP1. For the purposes of this study, we defined CL5 as extending from Lys^{486} to Leu^{545} (Fig. 1*A*). This CL5 sequence is identical in all reported mammalian orthologs (mouse, rat, chicken, dog, cow, and monkey) of MRP1 and contains a high abundance of ionizable amino acids. These residues do not appear to be randomly distributed, but rather, many occur in "clusters" creating ionic "patches" in this region of MRP1/Mrp1. Among the eight CL5 residues initially targeted in this study, four (Arg^{501}, Lys^{516}, Arg^{532}, and Glu^{535}) are identical in all ABCC subfamily homologs (Fig. 1*A*), whereas Glu^{507} and Glu^{521} are identical in 11 of 12 family members. The Lys residues at positions 503 and 513 are also highly conserved, although Arg is often found in their place.

The α-helices extending from TM9 and TM10 into the cytoplasm are linked by a stretch of amino acids (residues 507–521) that comprise the CL5 interface with NBD2 and also contain the so-called "coupling helix," which is presumably initiated by Gly^{511} (Fig. 1*A*) (10, 11). Gly^{511} is moderately con-

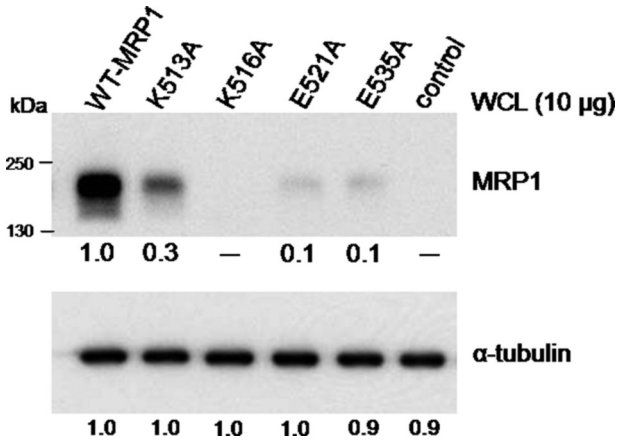

FIGURE 2. **Levels of Ala-substituted MRP1 mutant proteins of Lys^{513}, Lys^{516}, Glu^{521}, and Glu^{535}.** Shown is a representative immunoblot of whole cell lysates (*WCL*) (10 μg of protein/*lane*) prepared from HEK293T cells transfected with wild-type (WT-MRP1) and mutant (K513A, K516A, E521A, and E535A) cDNA expression vectors. Untransfected cells were used as a negative control. MRP1 proteins were detected with mAb QCRL-1 (*top*), and the relative levels, estimated by densitometry, are indicated *below* the blot (after correction for loading based on α-tubulin levels detected using an anti-α-tubulin mAb (*bottom*)). Similar values were obtained with cell lysates prepared from three independent transfections.

served and is present in the analogous positions of MRP1–4 and -7, ABCC8/SUR1, and ABCC9/SUR2 as well as the bacterial Sav1866. However, Tyr is found in MRP5/ABCC5, Asn in ABCC6/MRP6 and CFTR, and Cys in ABC11/MRP8 and ABCC12/MRP9 (Fig. 1*A*).

Charged Amino Acids in CL5 are Critical for Membrane Expression of MRP1—The role of the eight charged residues in CL5 for the plasma membrane expression of MRP1 in mammalian cells was initially investigated by comparing MRP1 protein levels in lysates of HEK293T cells transfected with cDNA expression vectors encoding Ala-substituted mutants. Densitometric analysis of immunoblots showed that the K516A, E521A, and E535A mutants were consistently expressed very poorly (levels <10% of wild-type MRP1), whereas the levels of K513A were reduced by >70% (Fig. 2). These observations indicate that substitution of Lys^{513}, Lys^{516}, Glu^{521}, and Glu^{535} with the neutral, cavity-creating Ala has a deleterious effect on MRP1 levels, at least in mammalian cells. On the other hand, levels of the four remaining CL5 Ala-substituted mutants (R501A, K503A, E507A, and R532A) were comparable with wild-type MRP1 (see Fig. 6*A*).

Effect of Reduced Temperature on Levels and Localization of Ala-substituted Lys^{513}, Lys^{516}, Glu^{521}, and Glu^{535} Mutants—Misfolded proteins are frequently targeted for degradation by the endoplasmic reticulum-associated degradation (ERAD) pathways (37, 38). However, levels of misfolded mutant proteins can often be enhanced by diminishing the activity of ERAD pathways by incubating cells expressing the mutants at subphysiological temperatures (20, 39, 40). When HEK cells containing the four poorly expressed Ala-substituted Lys^{513}, Lys^{516}, Glu^{521}, and Glu^{535} mutants were incubated at 28 °C rather than 37 °C, immunoblots of cell lysates showed two bands for wild-type MRP1, a band at 190 kDa (*band A*, fully glycosylated mature MRP1) and a second band at 170 kDa (*band B*, underglycosylated MRP1) (Fig. 3*A*). A marked increase in the levels of the K513A, K516A, E521A, and E535A mutants was observed in cells incubated at the lower temperature; however, most of this increase was attributable to the underglycosylated form of the MRP1. Furthermore, despite the increase, the levels of K513A, K516A, E521A, and E535A

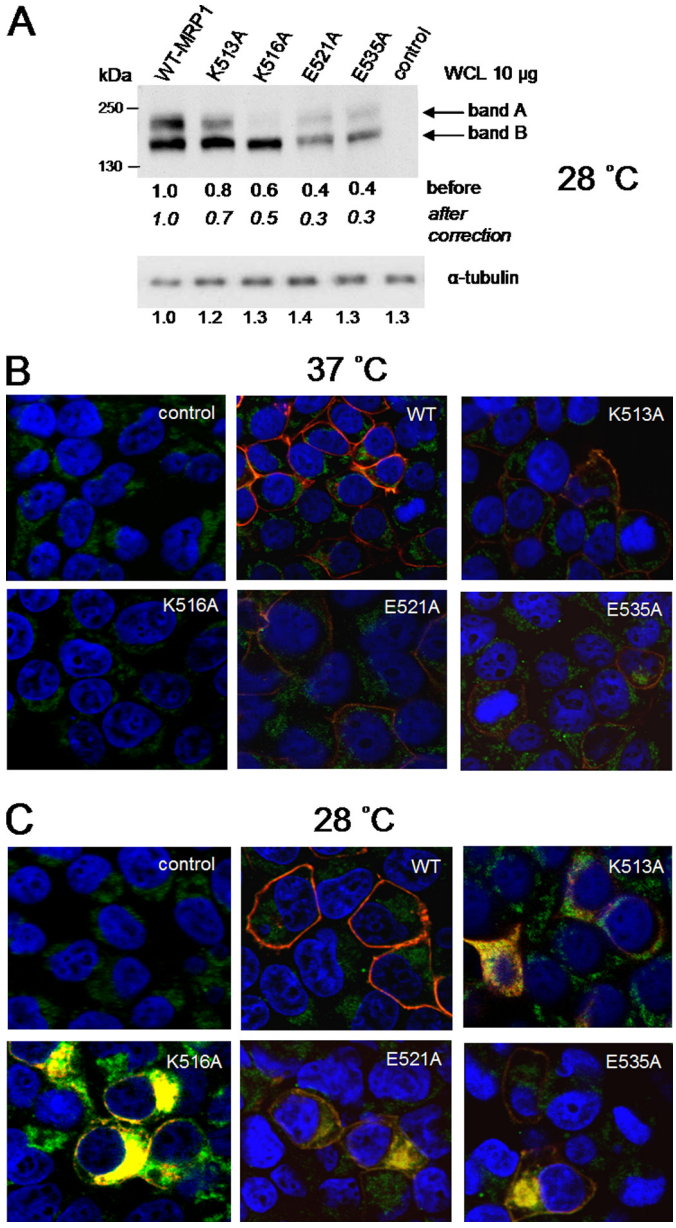

FIGURE 3. **Levels and localization of CL5 mutant MRP1 proteins.** *A*, immunoblots of whole cell lysates (*WCL*) (10 μg of protein/*lane*) prepared from HEK293T cells incubated at 28 °C for 60 h after transfection with mutant (K513A, K516A, E521A, and E535A) and wild-type MRP1 cDNA expression vectors. *Top*, MRP1 was detected with mouse mAb QCRL-1. *Band A* represents the 190-kDa fully glycosylated mature form of MRP1 and *band B* represents the 170-kDa underglycosylated immature form. Relative expression levels (mature and immature combined) before and after correction for protein loading based on α-tubulin levels are shown below. *B* and *C*, confocal microscopy of transfected HEK293T cells after incubation at 37 and 28 °C, respectively, for 48 h. Cells were analyzed by indirect immunofluorescence with MRP1-specific rat mAb MRPr1 (*red*) and mouse anti-calnexin mAb (*green*) binding detected with Alexa Fluor 546- and Alexa Fluor 488-conjugated secondary antibodies, respectively. Nuclei were stained with DAPI (*blue*). Signals from the three channels were acquired independently, and the merged images are presented. Co-localization of MRP1 and calnexin is indicated by a *yellow* color. *Control*, untransfected HEK293T cells.

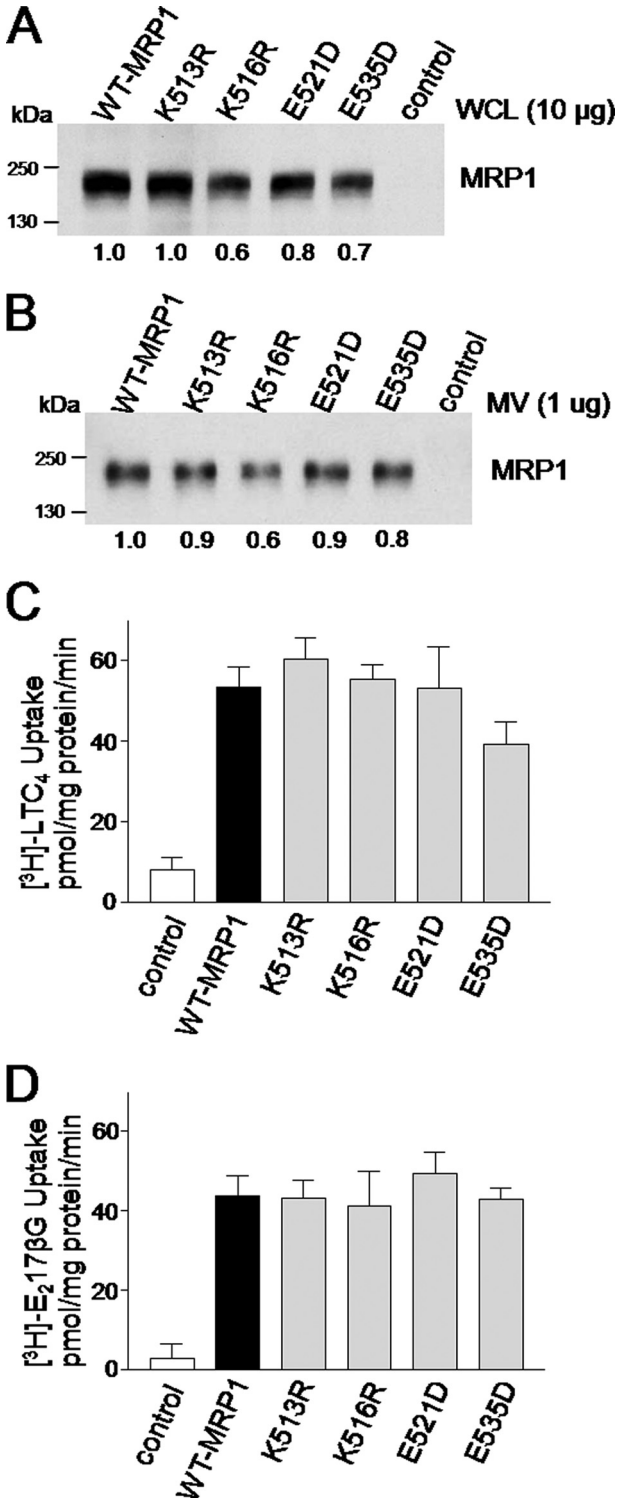

FIGURE 4. **Levels and organic anion transport by same charge Lys^{513}, Lys^{516}, Glu^{521}, and Glu^{535} mutants of MRP1.** *A* and *B*, representative immunoblots of whole cell lysates (*WCL*) (10 μg of protein/*lane*) (*A*) and membrane vesicles (1 μg of protein/*lane*) (*B*) prepared from HEK293T cells transfected with wild-type (WT-MRP1) and mutant (K513R, K516R, E521D, and E535D) MRP1 cDNA expression vectors. Untransfected cells were used as a negative control. MRP1 levels were detected with mAb QCRL-1, and the relative protein expression levels, estimated by densitometry, are shown *below* the blots. Similar values were obtained with whole cell lysates from a second independent transfection. *C* and *D*, ATP-dependent uptake of [^{3}H]LTC$_4$ (*C*) and [^{3}H]E$_2$17βG (*D*) by the membrane vesicles shown in *B* were determined, and values were adjusted to take into account any differences in MRP1 protein expression. The results shown are means ± S.D. of triplicate determinations in a single experiment. Similar results were obtained in at least one additional experiment with vesicles prepared from independently transfected cells.

remained substantially below those of the wild-type protein in membrane vesicle preparations from cells incubated at 28 °C (data not shown). The low levels of the mutant proteins precluded their functional characterization in vesicular transport assays.

Cells incubated at 37 and 28 °C were also examined by confocal microscopy, and the images obtained were consistent with the immunoblotting data of whole cell lysates (Figs. 2 and 3*A*). Thus, at 37 °C the MRP1 signals from cells expressing the K513A, E521A, and E535A mutants were very faint; however, the signals were found mostly at the plasma membrane as observed for wild-type MRP1 (Fig. 3*B*). This suggests that even if these mutations result in misfolding of MRP1, at least a minor portion is able to exit the endoplasmic reticulum and traffic normally to the plasma membrane. In contrast, K516A was not detectable at all in the HEK cells at 37 °C, suggesting that the misfolding of this mutant is so severe that none of this mutant protein escapes the ERAD pathways of the cell. On the other hand, when cells were incubated at 28 °C, the amount of mutant proteins increased (more so for K513A and K516A than for E521A and E535A) (Fig. 3, *A* and *C*). However, the MRP1 signals of all four mutants co-localized with calnexin, suggesting that at this temperature, the mutants are retained in the endoplasmic reticulum but presumably not degraded because of the diminished activity of the ERAD pathways at this subphysiological temperature. Although the "rescue" of K516A and K513A was greater than for E521A and E535A (Fig. 3*A*), the retention of K516A and K513A in the endoplasmic reticulum was more pronounced, whereas a small amount of E521A and E535A could be detected at the plasma membrane (Fig. 3*C*).

Expression and Transport Activity of "Same Charge" Mutants of Lys^{513}, Lys^{516}, Glu^{521}, and Glu^{535}—To determine whether it was the charge or another property of the amino acid at positions 513, 516, 521, and 535 that was critical for efficient plasma membrane expression of MRP1, same charge mutants (K513R, K516R, E521D, and E535D) were created and again expressed in HEK cells. At 37 °C, levels of the K513R mutant were comparable with wild-type MRP1 levels, whereas levels of the K516R, E521D, and E535D mutants were somewhat reduced (20–40%) (Fig. 4*A*). The transport properties of the same charge mutants were then examined using membrane vesicles prepared from the transfected cells (Fig. 4*B*). As shown in Fig. 4, *C* and *D*, levels of LTC$_4$ and E$_2$17βG transport by all four mutants were comparable with those of wild-type MRP1 (after correcting for relative MRP1 protein expression levels). Thus, the maintenance of the charge at amino acid positions 513, 516, 521, and 535 appears sufficient to retain the expression and transport function of MRP1.

Mutagenesis Guided by Analysis of a Homology Model of MRP1—For insight into how the above mutations might impair MRP1 protein expression, we examined the atomic environment of the expression-sensitive CL5 residues Lys^{513}, Lys^{516}, Glu^{521}, and Glu^{535} predicted by a homology model of

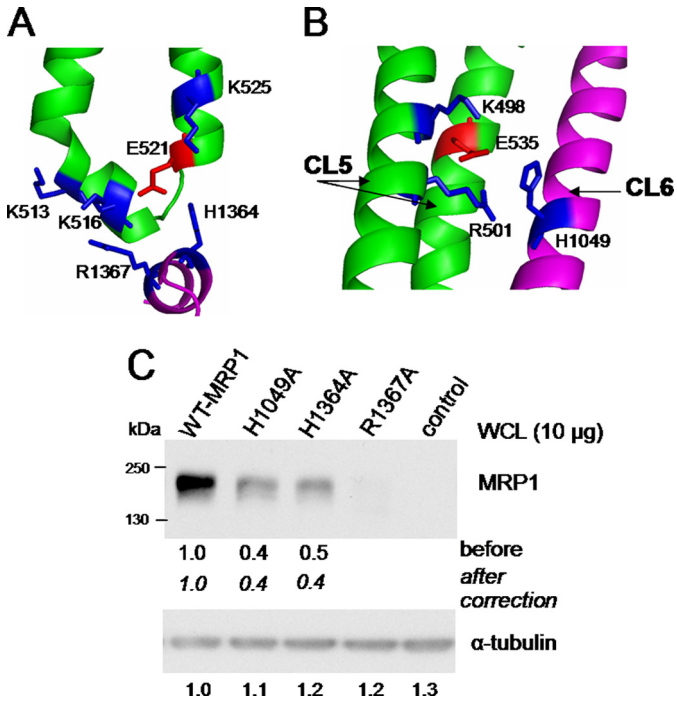

FIGURE 5. **Homology models and levels of MRP1 mutants H1049A, H1364A, and R1367A.** *A* and *B*, predicted location (relative to CL5) of His^{1364} and Arg^{1367} in NBD2 (*A*) and His^{1049} in CL6 (*B*) according to a homology model of the core region of MRP1 (11). *A* and *B* were created using PyMOL. *C*, representative immunoblot of whole cell lysates (*WCL*) (10 μg of protein/*lane*) prepared from HEK293T cells transfected with wild-type MRP1 and mutant cDNA expression vectors. Untransfected cells were used as a negative control. MRP1 was detected with mAb QCRL-1 (*top*), and relative levels before and after correction for protein loading based on α-tubulin levels are shown *below* the blot.

the core structure of MRP1 (11). Three of these residues (Lys^{513}, Lys^{516}, and Glu^{521}) cluster at the CL5 interface region that is predicted to come in close proximity to two highly conserved amino acids in NBD2 (His^{1364} and Arg^{1367}) (Fig. 5*A*). In our model, the side chain of CL5-Glu^{521} is predicted to be just 3.3 Å away from the side chain of NBD2-His^{1364}, a distance that would allow bonding interactions between these two domains, which we speculated might contribute to the correct folding and assembly of MRP1. Furthermore, Lys^{513} and Lys^{516} line up with Arg^{1367} at the CL5-NBD2 interface to form a positive ionic patch, which might also promote proper protein folding and hence membrane expression (11, 41). Our homology model also suggests that the side chain of the fourth expression-sensitive amino acid, Glu^{535} (which lies outside the CL5/NBD2 interface region), could come in close proximity with the side chains of CL5 Arg^{501} (at the juxtamembrane region of TM9) and His^{1049} (in CL6) to participate in interhelical interactions (based on estimated atomic distances of 3.1 and 4.2 Å between the potential interacting atoms) (Fig. 5*B*).

The above analyses prompted us to hypothesize that, based on their proximity to an expression-sensitive residue of CL5, NBD2 residues His^{1364} and Arg^{1367} and CL6 residue His^{1049} could be important for MRP1 expression. We reasoned that bonding interactions between the different domains of MRP1 could aid in the proper folding and assembly of the transporter. To test this hypothesis, mutants H1049A, H1364A, and R1367A were generated, and the levels of the mutant proteins in HEK293T cells determined as described above. As observed for the CL5 mutant K516A, the NBD2 mutant R1367A was not detectable by immunoblot analysis (Fig. 5*C*). The levels of the NBD2 mutant H1364A and the CL6 mutant H1049A were also reduced by >50%. Thus, our model-based analysis of the atomic environment of the expression-sensitive CL5 amino acids led us to identify additional expression-sensitive residues in NBD2 (His^{1364} and Arg^{1367}) and CL6 (His^{1049}). Together, these findings lend support to the idea that interactions between the ionizable residues at the CL5-NBD2 interface and between CL5 and CL6 are critical for the proper assembly and membrane expression of MRP1 in mammalian cells.

Effect of Ala substitution of Arg^{501}, Lys^{503}, Glu^{507}, and Arg^{532} on MRP1 Transport Activity—As mentioned earlier, levels of the Ala-substituted mutants of Arg^{501}, Lys^{503}, Glu^{507}, and Arg^{532} were comparable with that of wild-type MRP1 (Fig. 6*A*), and the mutant proteins all routed correctly to the plasma membrane (results not shown). When their transport properties were examined, however, a 50–60% decrease in the [^{3}H]LTC_4 and [^{3}H]$E_2$17βG transport levels of the R501A, E507A, and R532A mutants was observed (Fig. 6, *B* and *C*). In contrast, the transport activity of K503A was comparable with wild-type MRP1, and therefore this mutant was not investigated further.

The reduced $E_2$17βG transport activity of the R501A, E507A, and R532A mutants was analyzed further by determining the kinetic parameters of uptake; the results of these experiments are summarized in Table 1. Comparable with earlier reports (22), wild-type MRP1 transported [^{3}H]$E_2$17βG with a K_m and V_{max} of 5.4 μM and 1088 pmol mg^{-1} min^{-1}, respectively. In contrast, the K_m ($E_2$17βG) values for the R501A, E507A, and R532A mutants were increased 3–5-fold (18–25 μM). The V_{max} values of these mutants were similar to wild-type MRP1. These results indicate that reduced $E_2$17βG transport by these CL5 mutants can be attributed to a decreased apparent uptake affinity for this substrate.

Effect of Mutation G511I on MRP1 Expression and Function—Analyses of our homology model of MRP1 also suggested that substitution of the sterically unencumbered Gly^{511} with a bulky β-branched amino acid like Ile could affect the geometry and/or mobility of CL5. If true, then such a mutation could also perturb interactions at the CL5/NBD2 interface and thus affect MRP1 folding, expression, and/or function. As shown in Fig. 7*A*, substitution of Gly^{511} with Ile had no effect on MRP1 protein levels; however, transport of LTC_4 and $E_2$17βG by the G511I mutant was decreased by ~60 and 75%, respectively (Fig. 7, *B* and *C*). These observations support the idea that Gly^{511} does not play a role in the proper assembly of MRP1 but rather may affect its substrate interactions.

The reduced transport activity of the G511I mutant could be caused by a reduction in substrate affinity or transport capacity. Because of the very low levels of $E_2$17βG transport by G511I, the apparent affinity (K_m) of this mutant for $E_2$17βG could not be determined directly by kinetic analysis. Therefore, the affinity for this conjugated estrogen was measured indirectly by testing its ability to compete for [^{3}H]LTC_4 up-

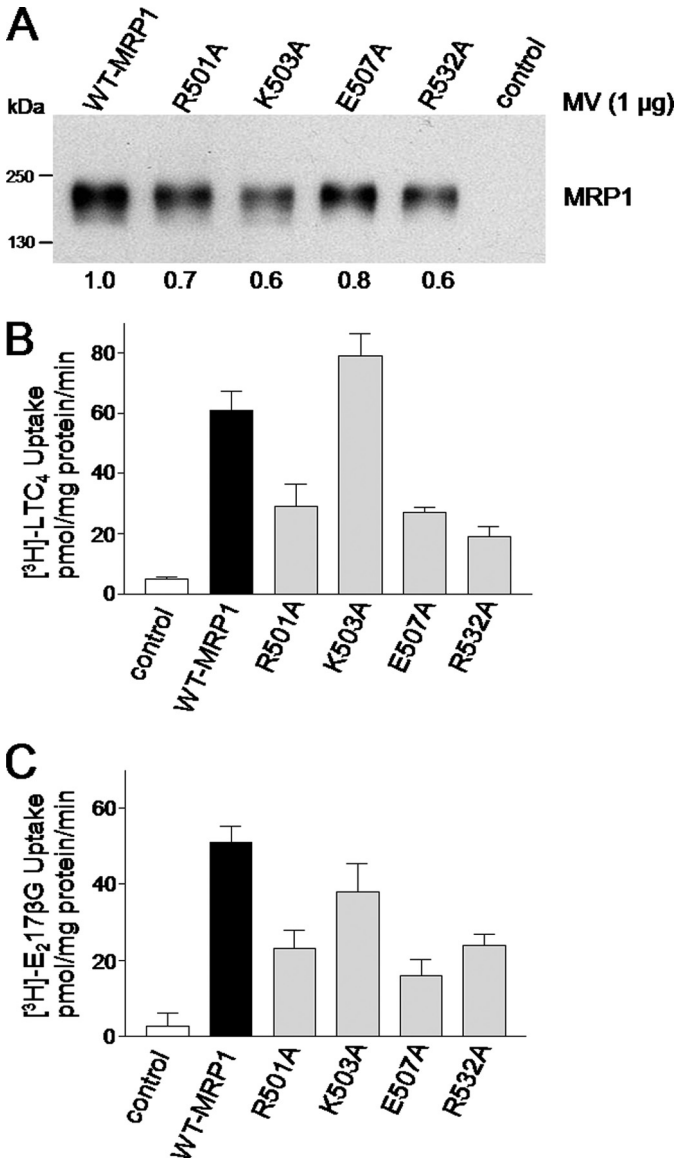

FIGURE 6. **Levels and organic anion transport activity of MRP1 mutant proteins R501A, K503A, E507A, and R532A.** *A*, shown is a representative immunoblot of membrane vesicles (*MV*) (1 μg of protein/*lane*) prepared from HEK293T cells transfected with wild-type (WT-MRP1) and mutant (R501A, K503A, E507A, and R532A) cDNA expression vectors. Untransfected cells were used as a negative control. MRP1 was detected with mAb QCRL-1, and the relative protein expression levels were estimated by densitometry and are shown below the blot. Similar values were obtained with vesicles prepared from 2–3 additional independent transfections. *B* and *C*, ATP-dependent uptake of [^{3}H]LTC$_4$ (*B*) and [^{3}H]E$_2$17βG (*C*) by the membrane vesicles shown in *A* were determined and values adjusted to take into account any differences in MRP1 protein levels. The results shown are means ± S.D. of triplicate determinations in a single experiment. Similar results were obtained in at least two additional experiments with vesicles derived from independent transfections.

take into inside-out membrane vesicles. As shown in Fig. 7*D*, E$_2$17βG inhibited [^{3}H]LTC$_4$ uptake by G511I and wild-type MRP1 with IC$_{50}$ values that differed by 5-fold (40 *versus* 8 μM, respectively). The ability of LTC$_4$ to inhibit [^{3}H]E$_2$17βG uptake by the G511I mutant relative to wild-type MRP1 was also reduced, as reflected by an ~3-fold difference in the IC$_{50}$ values (Fig. 7*E*). These observations support the conclusion that decreased transport by the G511I mutant is caused by a reduction in substrate affinity.

TABLE 1

Kinetic parameters of E$_2$17βG uptake by MRP1 mutants R501A, E507A, and R532A

K_m and V_{max} values for E$_2$17βG uptake by membrane vesicles (4 μg of protein) prepared from HEK293T cells transfected with wild-type or mutant proteins were determined by measuring ATP-dependent uptake at eight different E$_2$17βG concentrations (0.25–25 μM) for 1 min at 37 °C as described under "Experimental Procedures." Kinetic parameters were calculated by nonlinear regression and Michaelis-Menten analyses. The values shown are means of triplicate determinations in a single experiment and are representative of results obtained in three independent experiments.

Transfectant	K_m	V_{max}[a]	$(V_{max}/K_m) \times 10^{-3}$
	μM	*pmol/mg/min*	*mg/liter/min*
WT-MRP1	5.4	1088	0.20
R501A	22.9	1274	0.05
E507A	18.1	1150	0.06
R532A	24.5	1031	0.04

[a] V_{max} values have been corrected for differences in protein expression of the mutants relative to WT-MRP1 (Fig. 7*A*).

Photolabeling of MRP1 Mutants R501A, E507A, R532A, and G511I with [^{3}H]LTC$_4$—To determine whether the decrease in LTC$_4$ uptake by the R501A, E507A, R532A, and G511I mutants was associated with decreased binding of this substrate to MRP1, membrane vesicles enriched for wild-type or mutant MRP1 were photolabeled with [^{3}H]LTC$_4$. As shown in Fig. 8*A*, [^{3}H]LTC$_4$ labeling of the R501A and E507A mutants was decreased by 50%, whereas labeling of the R532A mutant was decreased by 70%. Labeling of the G511I mutant by [^{3}H]LTC$_4$ was also reduced by 40% (Fig. 8*B*) (after correcting for differences in protein levels). These relative levels of photolabeling correlated well with the relative LTC$_4$ transport activities of these mutants and, in the case of G511I, with the reduced affinity for this substrate suggested by the competition experiments (Fig. 7*E*).

Photolabeling of Mutants E507A and G511I with 8-Azido-[α-^{32}P]ATP and Orthovanadate- and BeF-induced Trapping of 8-Azido-[α-^{32}P]ADP—The precise role of the CLs in coupling the ATPase activity of ABC transporters to the translocation of their substrates is not yet fully understood (12, 42). Of the four CL5 mutants that showed reduced transport activity, two of them (Glu^{507} and Gly^{511}) are expected to be part of CL5 region that interfaces with NBD2; therefore, these residues would be well positioned to be involved in mediating signaling between the catalytic activity at the NBDs and the substrate translocation through the MSDs. For this reason, the interactions of the transport-deficient E507A and G511I mutants with ATP were examined. First, ATP binding was measured by photolabeling the mutant proteins with 8-azido-[α-^{32}P]ATP under conditions of minimal hydrolysis. As shown in Fig. 9*A*, no significant differences between the photolabeling of the mutants and wild-type MRP1 were observed. Next, the catalytic activity of the E507A and G511I mutants was examined by measuring the amount of azido-[^{32}P]ADP trapped by orthovanadate under conditions permissive for ATP hydrolysis (26). As shown in Fig. 9*B*, [^{32}P]ADP trapping by the G511I mutant was reduced by 40%, whereas trapping by the E507A mutant was comparable to wild-type MRP1. Similar results were observed when beryllium fluoride instead of orthovanadate was used to trap azido-[^{32}P]ADP (data not shown).

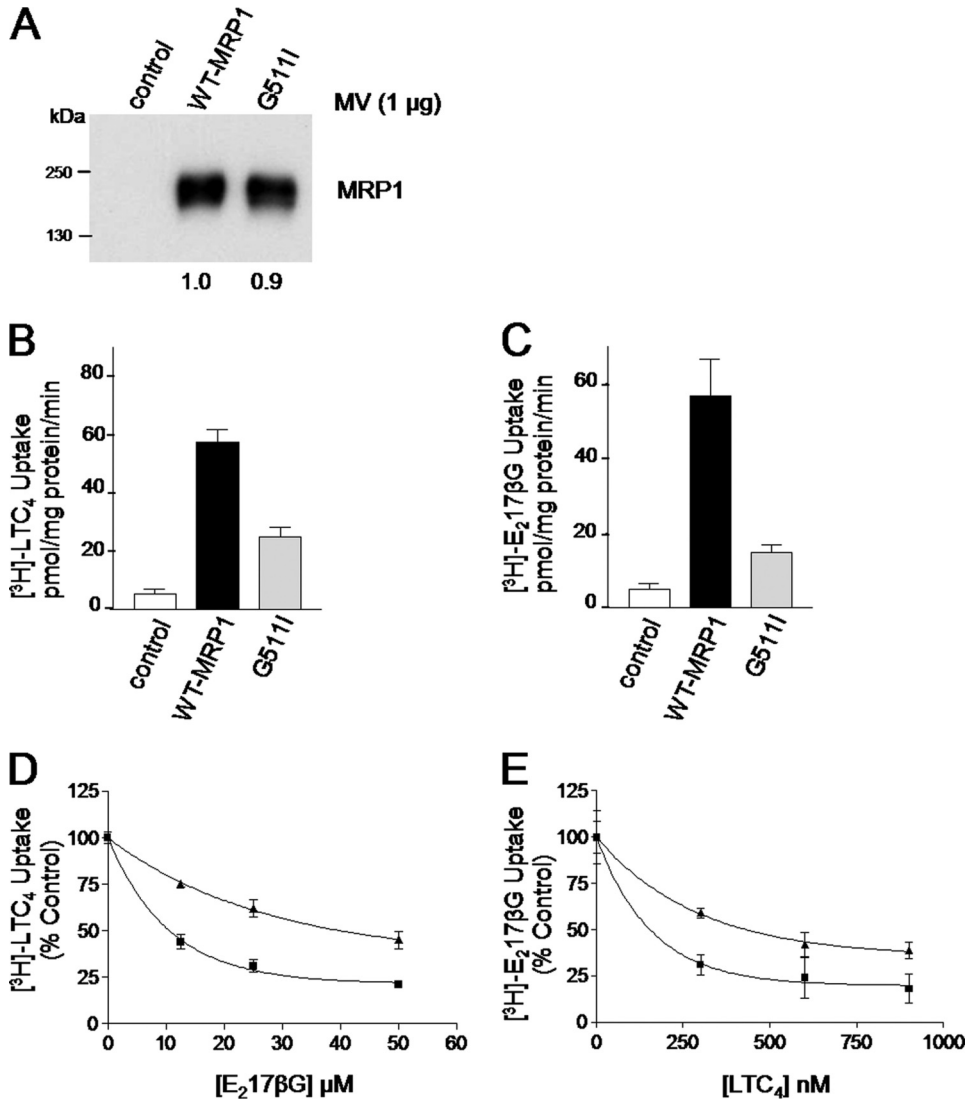

FIGURE 7. **Protein expression, transport activity, and inhibition of [^{3}H]LTC_4 and[^{3}H]$E_2$17βG uptake by wild-type MRP1 and mutant G511I.** *A*, immunoblot of membrane vesicles (1 μg of protein/*lane*) prepared from HEK293T cells transfected with wild-type MRP1 and mutant G511I cDNA expression vectors. MRP1 proteins were detected with mAb QCRL-1, and the relative expression levels are shown *below* the blot. Similar values were obtained with vesicles from 2–3 additional independent transfections. *B* and *C*, ATP-dependent uptake of [^{3}H]LTC_4 and [^{3}H]$E_2$17βG by the membrane vesicles shown in *A* were determined, and values were corrected to take into account the difference in MRP1 protein expression. The results shown are means ± S.D. of triplicate determinations in a single experiment. Similar results were obtained in at least two additional experiments with vesicles derived from independent transfections. *D* and *E*, membrane vesicles prepared from HEK293T cells transfected with wild-type (■, WT-MRP1) and mutant (▲, G511I) MRP1 cDNA expression vectors were incubated for 1 min with either [^{3}H]LTC_4 at 23 °C in the presence of $E_2$17βG (0, 12.5, 25, and 50 μM) (*D*) or [^{3}H]$E_2$17βG at 37 °C in the presence of LTC_4 (0, 300, 600, and 900 nM) (*E*). The results, expressed as a percentage of transport activity in the absence of competitive substrate, are means ± S.D. of triplicate determinations in a single experiment. Similar results were obtained in a second independent experiment.

DISCUSSION

In the present study, mutational analyses of selected amino acids in CL5 of MSD1 and NBD2 were conducted to investigate the potential role of CL5 itself as well as the interface between these two domains in determining both the expression and activity of MRP1. Initially, mutations of the eight most conserved charged amino acids in CL5 as well as the helix-disrupting Gly^{511} were generated, and the consequences on MRP1 expression and transport activity were evaluated. Of the charged amino acid mutants, only K503A exhibited properties comparable with those of wild-type MRP1, whereas the seven remaining Ala-substituted mutants were either poorly expressed (K513A, K516A, E521A, and E535A) or exhibited significantly reduced transport activity (R501A, E507A, and R532A). LTC_4 and $E_2$17βG transport by the G511I mutant was also reduced, although their expression levels were comparable with wild-type MRP1. Together, these results illustrate the remarkable sensitivity of CL5 to mutation and thus establish its critical role in the expression and function of MRP1. Amino acids that are important for expression or function of a protein are usually well conserved (41, 43), and based on the results presented here, it is clear that this holds true for MRP1 as well.

The substantially reduced levels of the K513A, K516A, E521A, and E535A mutants indicates that introducing a neutral cavity-creating Ala residue at these positions is not compatible with some aspect(s) of MRP1 biosynthesis or assembly, at least in HEK cells. When cells transfected with the

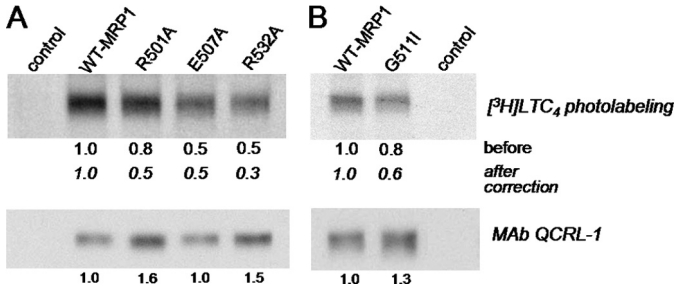

FIGURE 8. **[^{3}H]LTC$_4$ photolabeling of wild-type and MRP1 mutants R501A, E507A, R532A, and G511I.** *A* and *B*, membrane vesicles (50 μg of protein/*lane*) prepared from transfected HEK293T cells were incubated with [^{3}H]LTC$_4$ (200 nM, 120 nCi) at room temperature for 30 min, irradiated at 302 nm, and then resolved by SDS-PAGE and processed for fluorography. Band intensities were determined by densitometry, and relative levels of photolabeling were calculated after correction for differences in MRP1 levels as detected with mAb QCRL-1 (*bottom*).

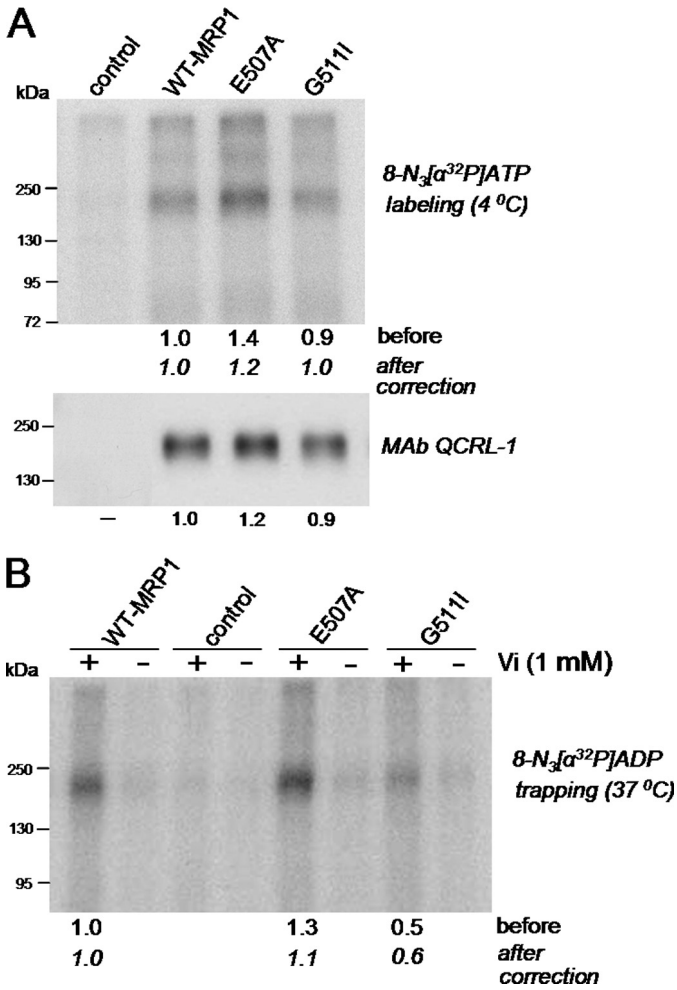

FIGURE 9. **Azido-[^{32}P]ATP labeling and vanadate-induced trapping of azido-[^{32}P]ADP by E507A and G511I mutant MRP1 proteins.** *A*, membrane vesicles (20 μg of protein) from transfected cells were incubated with 5 μM 8-azido-[α-^{32}P]ATP on ice for 5 min in transport buffer containing 5 mM $MgCl_2$. Samples were irradiated at 302 nm and, after removal of unincorporated nucleotides, resolved by SDS-PAGE. The gel was dried and then exposed to film. Relative band intensities were analyzed by densitometry and are indicated by the *numbers* below the *lanes*, expressed before and after correction for differences in MRP1 protein levels (*bottom*). *B*, vanadate-induced trapping of azido-[^{32}P]ADP was measured by incubating membrane vesicles (20 μg of protein) at 37 °C with 8-azido-[α-^{32}P]ATP in the presence (+) or absence (−) of orthovanadate for 15 min in transport buffer. Samples were irradiated and processed as described under "Experimental Procedures." Similar results were obtained in at least two additional independent experiments.

poorly expressed mutant MRP1 cDNA expression vectors were incubated at a subphysiological temperature, marked increases in the levels of the K513A, K516A, E521A, and E535A mutants were observed, although they remained well below those of wild-type MRP1 and consisted of both mature and underglycosylated forms of the transporter. The mutant proteins were also largely retained in the endoplasmic reticulum at 28 °C, presumably reflecting a diminished activity of the ERAD pathways. Underglycosylation of the mutants is not responsible for the retention in the endoplasmic reticulum, as both under- and fully glycosylated wild-type MRP1 trafficked normally to the plasma membrane at 28 °C, consistent with previous reports that this post-translational modification is not critical for the trafficking or function of MRP1 (9, 44, 45).

The three expression-sensitive CL5 amino acids (Lys^{513}, Lys^{516}, and Glu^{521}) together with His^{1364} and Arg^{1367} in NBD2 are predicted to form a cluster of charged residues at the interface of the two domains, which led us to hypothesize that these amino acids might play an important role in maintaining the integrity of the interface between CL5 and NBD2 that is needed for normal expression of MRP1. This hypothesis was supported by our observations that MRP1 expression is retained when the three CL5 residues are replaced with same charge amino acids but is lost or reduced when either the NBD2 residue Arg^{1367} or His^{1364} is replaced with Ala. Of relevance to our findings is a recent cross-linking study of Cys-substituted mutants of the Abcc-related yeast transporter Yor1p in which it was demonstrated that Tyr^{403} in CL2 (analogous to Leu^{517} in CL5 of MRP1) is within bonding distance of multiple amino acids within NBD2; this was interpreted as evidence that the interface between NBD2 and CL2 is robust (46). If interdomain-stabilizing bonding interactions do indeed exist between CL5 and NBD2 of MRP1, the observation that the decrease in MRP1 levels is more pronounced for the Glu^{521} mutant than for the His^{1364} mutant suggests that they are not exclusive. Indeed, homology models indicate the potential existence of multiple intrahelical and interhelical interactions for CL5 Glu^{521}. In light of this finding, it is perhaps not surprising that MRP1 levels remained low in the reciprocal double exchange mutant E521H/H1364E (data not shown).

The fourth expression-sensitive CL5 amino acid, Glu^{535}, resides in the distal end of the loop close to the juxtamembrane region of TM10, where our model suggests it could participate in bonding interactions with Lys^{498} and Arg^{501} in CL5 and the side chain of His^{1049} in CL6. If such interdomain interactions exist and are important for the proper folding and assembly of MRP1, it was reasonable to expect that, as we observed for the Ala substitution of Glu^{535}, replacing His^{1049} with Ala would also affect the levels of MRP1. Indeed, this was the case, although the reduction in E535A protein levels was significantly greater (>90%) than the reduction observed for H1049A (60%). Ala substitutions of Arg^{501} also resulted in reduced MRP1 levels, indicating that Glu^{535} is likely involved in multiple bonding interactions, some or

all of which could contribute to the proper folding of MRP1 protein.

The importance of maintaining the integrity of CL5 and its interface with NBD2 as well as its interaction with CL6 for proper expression and assembly of MRP1 appears likely to be a conserved feature of several other mammalian ABCC transporters. For example, mutations that cause the connective tissue disorder known as pseudoxanthoma elasticum are found throughout the *ABCC6/MRP6* gene (47), but relevant to the results presented here are the disease-associated mutations of ABCC6-Lys^{502} (analogous to MRP1-Lys^{516}) and ABCC6-Arg^{1339} (analogous to MRP1-Arg^{1367}). Similarly, a deletion mutation (ΔE278) and two missense mutations (R258G and E292K) in CFTR/ABCC7 that involve amino acids analogous to MRP1-Glu^{521}, -Arg^{501}, and -Glu^{535}, respectively, are associated with cystic fibrosis (48).

In contrast to the Ala substitutions of Lys^{513}, Lys^{516}, Glu^{521}, and Glu^{535}, Ala substitutions of Arg^{501}, Lys^{503}, Glu^{507}, and Arg^{532} had no substantial effect on MRP1 levels in HEK cells. Nevertheless, although the K503A mutant exhibited properties similar to wild-type MRP1, the LTC_4 and $E_2$17βG transport activities of R501A, E507A, and R532A were significantly reduced. Kinetic analyses and photolabeling studies indicated that the decreased transport activity of these three mutants could be attributed largely to a reduced affinity for their substrates. Because it is widely held that the substrate binding sites of ABC transporters are located in the TMs (12, 42), the possibility that Arg^{501}, Glu^{507}, and Arg^{532} are not directly involved in the binding of MRP1 substrates must be considered. However, these amino acids reside in the cytoplasmic α-helical extensions of TM9 (Arg^{501} and Glu^{507}) and TM10 (Arg^{532}), and consequently it is conceivable that replacing these residues with the cavity-creating Ala could perturb the geometry of the respective TM helices. This in turn could indirectly affect the affinity with which MRP1 binds and transports its substrates, $E_2$17βG and LTC_4. Again, relevant to our present work, Pagant *et al.* (46) recently reported that although mutation of Arg^{387} in Yor1p (analogous to Arg^{501} in MRP1) have no effect on plasma membrane trafficking of this yeast transporter, the mutant protein no longer confers resistance to oligomycin. In addition, unlike wild-type Yor1p, TM6 and TM12 of the Yor1p-R387G mutant could no longer be cross-linked. Thus the authors concluded that although the Arg^{387} mutation clearly alters the conformation of Yor1p, the change is not sufficient to activate the ERAD pathways.

With the flexibility afforded by the absence of a side chain, Gly^{511} seems the most likely amino acid to initiate the first turn in CL5 to facilitate the linking of TM9 with TM10. By replacing the freely rotating Gly with a bulky Ile, we anticipated that the geometry and mobility of CL5 would be altered, which could have an impact on the expression or function of MRP1. The fact that the G511I mutant was expressed at levels comparable with that of wild-type MRP1 suggests that even after the geometry of CL5 was altered, the integrity of its interface with NBD2 was not significantly altered. Nevertheless, the G511I mutant showed reduced transport activity, which was associated with an apparent decrease in substrate binding, again implicating a direct or indirect role for this region in substrate recognition by MRP1. However, it is worth noting that unlike the other functionally important residues identified in this study, Gly^{511} is only moderately conserved, and although present in MRP1–4 and -7 and SUR1 and -2 as well as Sav1866, it is not found in MRP5, ABCC6, CFTR, or Yor1p.

Given the predicted location of Glu^{507} and Gly^{511} at the interface of CL5 with NBD2, and thus their potential role in mediating signaling between the NBDs and MSDs during the transport process, it was of interest to determine whether the reduced transport activity observed after mutation of these two amino acids involved any changes in the interactions of MRP1 with nucleotide. Although binding of azido-[^{32}P]ATP by the mutants was not affected, vanadate-induced trapping of azido-[^{32}P]ADP was moderately reduced for G511I but not for E507A. This suggests that for the Glu^{507} mutant, changes in substrate affinity appear to be solely accountable for its reduced activity, whereas for the Gly^{511} mutant, changes in the catalytic activity of the transporter may also be involved. Thus, despite their close proximity to one another, these two amino acids play different roles in the function of MRP1.

Relevant to our findings described here are the properties of a double MRP1 mutant containing a Leu substitution of Glu^{507} and a Pro substitution of Gly^{511} (E507L/G511P) after expression in insect cells (reported by Ren *et al.* (49)). Unfortunately, direct comparisons are not possible because single Glu^{507} and Gly^{511} mutants were not investigated. Nevertheless, these authors reported that the LTC_4 transport activity of the double mutant was reduced by >80%, a larger decrease than we observed for either of the single E507A and G511I mutants. Thus the effects of the two mutations may be additive, which is consistent with our conclusion that the two amino acids play different roles in MRP1 function.

In summary, the present studies have firmly established that a cluster of charged residues (Lys^{513}, Lys^{516}, Glu^{521}, His^{1364}, and Arg^{1367}), which homology models predict to lie at the interface of CL5 with NBD2, play a critical role in the plasma membrane expression of human MRP1 in mammalian cells. When compared with our earlier investigations of CL7 in MSD2, our present data also indicate that CL5 in MSD1 plays a more prominent role in ensuring the plasma membrane expression of MRP1 than CL7. Furthermore, in contrast to transport-deficient CL7 mutants, the transport-deficient CL5 mutants described here show no apparent substrate selectivity, suggesting that more global conformational changes may be involved. Together, these observations point to a differential role for CL5 and CL7 in determining the membrane levels and function of MRP1 and provide further evidence of the structural and functional asymmetry of this transporter. Ongoing studies are focused on the exploration of different experimental strategies, including the use of chemical chaperones, to restore levels of the poorly expressing CL mutants as a means of understanding the molecular features that regulate the proper assembly and trafficking of MRP1 to the plasma membrane.

Acknowledgments—We thank Dr. Gwenaëlle Conseil for help in experimental methods and useful discussions and Kathy Sparks for technical assistance.

REFERENCES

1. Cole, S. P., Bhardwaj, G., Gerlach, J. H., Mackie, J. E., Grant, C. E., Almquist, K. C., Stewart, A. J., Kurz, E. U., Duncan, A. M., and Deeley, R. G. (1992) *Science* **258,** 1650–1654
2. Dean, M., and Allikmets., R. (2001) *J. Bioenerg. Biomembr.* **33,** 475–479
3. Cole, S. P., Sparks, K. E., Fraser, K., Loe, D. W., Grant, C. E., Wilson, G. M., and Deeley, R. G. (1994) *Cancer Res.* **54,** 5902–5910
4. Leslie, E. M., Deeley, R. G., and Cole, S. P. (2005) *Toxicol. Appl. Pharmacol.* **204,** 216–237
5. Deeley, R. G., Westlake, C., and Cole, S. P. (2006) *Physiol. Rev.* **86,** 849–899
6. Cole, S. P., and Deeley, R. G. (2006) *Trends Pharmacol. Sci.* **27,** 438–446
7. Wijnholds, J., Evers, R., van Leusden, M. R., Mol, C. A., Zaman, G. J., Mayer, U., Beijnen, J. H., van der Valk, M., Krimpenfort, P., and Borst, P. (1997) *Nat. Med.* **3,** 1275–1279
8. Borst, P., Evers, R., Kool, M., and Wijnholds, J. (2000) *J. Natl. Cancer Inst.* **92,** 1295–1302
9. Hipfner, D. R., Almquist, K. C., Leslie, E. M., Gerlach, J. H., Grant, C. E., Deeley, R. G., and Cole, S. P. (1997) *J. Biol. Chem.* **272,** 23623–23630
10. Dawson, R. J., and Locher, K. P. (2006) *Nature* **443,** 180–185
11. DeGorter, M. K., Conseil, G., Deeley, R. G., Campbell, R. L., and Cole, S. P. (2008) *Biochem. Biophys. Res. Commun.* **365,** 29–34
12. Locher, K. P. (2009) *Philos. Trans. R. Soc. Lond. B Biol. Sci.* **364,** 239–245
13. Deeley, R. G., and Cole, S. P. (2006) *FEBS Lett.* **580,** 1103–1111
14. Haimeur, A., Conseil, G., Deeley, R. G., and Cole, S. P. (2004) *Mol. Pharmacol.* **65,** 1375–1385
15. Koike, K., Oleschuk, C. J., Haimeur, A., Olsen, S. L., Deeley, R. G., and Cole, S. P. (2002) *J. Biol. Chem.* **277,** 49495–49503
16. Kwan, T., and Gros, P. (1998) *Biochemistry* **37,** 3337–3350
17. Oancea, G., O'Mara, M. L., Bennett, W. F., Tieleman, D. P., Abele, R., and Tampé, R. (2009) *Proc. Natl. Acad. Sci. U.S.A.* **106,** 5551–5556
18. Seibert, F. S., Jia, Y., Mathews, C. J., Hanrahan, J. W., Riordan, J. R., Loo, T. W., and Clarke, D. M. (1997) *Biochemistry* **36,** 11966–11974
19. Seibert, F. S., Linsdell, P., Loo, T. W., Hanrahan, J. W., Clarke, D. M., and Riordan, J. R. (1996) *J. Biol. Chem.* **271,** 15139–15145
20. Xie, J., Drumm, M. L., Ma, J., and Davis, P. B. (1995) *J. Biol. Chem.* **270,** 28084–28091
21. Conseil, G., Deeley, R. G., and Cole, S. P. (2005) *Biochem. Pharmacol* **69,** 451–461
22. Conseil, G., Deeley, R. G., and Cole, S. P. (2006) *J. Biol. Chem.* **281,** 43–50
23. Conseil, G., Rothnie, A. J., Deeley, R. G., and Cole, S. P. (2009) *Mol. Pharmacol.* **75,** 397–406
24. Gao, M., Cui, H. R., Loe, D. W., Grant, C. E., Almquist, K. C., Cole, S. P., and Deeley, R. G. (2000) *J. Biol. Chem.* **275,** 13098–13108
25. Hou, Y., Cui, L., Riordan, J. R., and Chang, X. (2000) *J. Biol. Chem.* **275,** 20280–20287
26. Koike, K., Conseil, G., Leslie, E. M., Deeley, R. G., and Cole, S. P. (2004) *J. Biol. Chem.* **279,** 12325–12336
27. Ito, K., Olsen, S. L., Qiu, W., Deeley, R. G., and Cole, S. P. (2001) *J. Biol. Chem.* **276,** 15616–15624
28. Hipfner, D. R., Gauldie, S. D., Deeley, R. G., and Cole, S. P. (1994) *Cancer Res.* **54,** 5788–5792
29. Hipfner, D. R., Mao, Q., Qiu, W., Leslie, E. M., Gao, M., Deeley, R. G., and Cole, S. P. (1999) *J. Biol. Chem.* **274,** 15420–15426
30. Loe, D. W., Almquist, K. C., Deeley, R. G., and Cole, S. P. (1996) *J. Biol. Chem.* **271,** 9675–9682
31. Létourneau, I. J., Deeley, R. G., and Cole, S. P. (2005) *Pharmacogenet. Genomics* **15,** 647–657
32. Sauna, Z. E., Müller, M., Peng, X. H., and Ambudkar, S. V. (2002) *Biochemistry* **41,** 13989–14000
33. Aller, S. G., Yu, J., Ward, A., Weng, Y., Chittaboina, S., Zhuo, R., Harrell, P. M., Trinh, Y. T., Zhang, Q., Urbatsch, I. L., and Chang, G. (2009) *Science* **323,** 1718–1722
34. Ravna, A. W., Sylte, I., and Sager, G. (2008) *Eur. J. Med. Chem.* **43,** 2557–2567
35. Zolnerciks, J. K., Wooding, C., and Linton, K. J. (2007) *FASEB J.* **21,** 3937–3948
36. Hazai, E., and Bikádi, Z. (2008) *J. Struct. Biol.* **162,** 63–74
37. Roth, J., Yam, G. H., Fan, J., Hirano, K., Gaplovska-Kysela, K., Le Fourn, V., Guhl, B., Santimaria, R., Torossi, T., Ziak, M., and Zuber, C. (2008) *Histochem. Cell Biol.* **129,** 163–177
38. Brodsky, J. L., and Wojcikiewicz, R. J. (2009) *Curr. Opin. Cell Biol.* **21,** 516–521
39. Cohen, B. D., Bariteau, J. T., Magenis, L. M., and Dias, J. A. (2003) *Endocrinology* **144,** 4393–4402
40. Dobson, C. M. (2003) *Nature* **426,** 884–890
41. Riordan, J. R. (2008) *Annu. Rev. Biochem.* **77,** 701–726
42. Seeger, M. A., and van Veen, H. W. (2009) *Biochim. Biophys. Acta* **1794,** 725–737
43. Skach, W. R. (2009) *Nat. Struct. Mol. Biol.* **16,** 606–612
44. Bakos, E., Hegedüs, T., Holló, Z., Welker, E., Tusnády, G. E., Zaman, G. J., Flens, M. J., Váradi, A., and Sarkadi, B. (1996) *J. Biol. Chem.* **271,** 12322–12326
45. Müller, M., Yong, M., Peng, X. H., Petre, B., Arora, S., and Ambudkar, S. V. (2002) *Biochemistry* **41,** 10123–10132
46. Pagant, S., Brovman, E. Y., Halliday, J. J., and Miller, E. A. (2008) *J. Biol. Chem.* **283,** 26444–26451
47. Li, Q., Jiang, Q., Pfendner, E., Váradi, A., and Uitto, J. (2009) *Exp. Dermatol.* **18,** 1–11
48. Mercier, B., Verlingue, C., Lissens, W., Silber, S. J., Novelli, G., Bonduelle, M., Audrézet, M. P., and Férec, C. (1995) *Am. J. Hum. Genet.* **56,** 272–277
49. Ren, X. Q., Furukawa, T., Yamamoto, M., Aoki, S., Kobayashi, M., Nakagawa, M., and Akiyama, S. (2006) *J. Biochem.* **140,** 313–318